

4-8-2015

Engineering of a light-gated potassium channel

Christian Cosentino

Universita degli Studi di Milano, cristian.cosentino@unimi.it

Laura Alberio

Universita degli Studi di Milano

Sabrina Gazzarrini

Universita degli Studi di Milano

Marco Aquila


Universita degli Studi di Milano

Eduardo Romano

Universita degli Studi di Milano

See next page for additional authors

Follow this and additional works at: <https://digitalcommons.unl.edu/vanetten>

 Part of the [Genetics and Genomics Commons](#), [Plant Pathology Commons](#), and the [Viruses Commons](#)

Cosentino, Christian; Alberio, Laura; Gazzarrini, Sabrina; Aquila, Marco; Romano, Eduardo; Cermenati, Solei; Zuccolini, Paolo; Petersen, Jan; Beltrame, Monica; Van Etten, James L.; Christie, John M.; Thiel, Gerhard; and Moroni, Anna, "Engineering of a light-gated potassium channel" (2015). *James Van Etten Publications*. 42.
<https://digitalcommons.unl.edu/vanetten/42>

This Article is brought to you for free and open access by the Plant Pathology Department at DigitalCommons@University of Nebraska - Lincoln. It has been accepted for inclusion in James Van Etten Publications by an authorized administrator of DigitalCommons@University of Nebraska - Lincoln.

Authors

Christian Cosentino, Laura Alberio, Sabrina Gazzarrini, Marco Aquila, Eduardo Romano, Solei Cermenati, Paolo Zuccolini, Jan Petersen, Monica Beltrame, James L. Van Etten, John M. Christie, Gerhard Thiel, and Anna Moroni

ral
ng
ze-
res
/a-
ar-
NA
ole

OPTOGENETICS

Engineering of a light-gated potassium channel

Cristian Cosentino,^{1*} Laura Alberio,¹ Sabrina Gazzarrini,¹ Marco Aquila,¹ Edoardo Romano,¹ Solei Cermenati,¹ Paolo Zuccolini,¹ Jan Petersen,² Monica Beltrame,¹ James L. Van Etten,³ John M. Christie,² Gerhard Thiel,⁴ Anna Moroni^{1†}

biol.
04).

The present palette of opsin-based optogenetic tools lacks a light-gated potassium (K⁺) channel desirable for silencing of excitable cells. Here, we describe the construction of a blue-light-induced K⁺ channel 1 (BLINK1) engineered by fusing the plant LOV2-J_α photosensory module to the small viral K⁺ channel Kcv. BLINK1 exhibits biophysical features of Kcv, including K⁺ selectivity and high single-channel conductance, but reversibly photoactivates in blue light. Opening of BLINK1 channels hyperpolarizes the cell to the K⁺ equilibrium potential. Ectopic expression of BLINK1 reversibly inhibits the escape response in light-exposed zebrafish larvae. BLINK1 therefore provides a single-component optogenetic tool that can establish prolonged, physiological hyperpolarization of cells at low light intensities.

3

ol.

41

540

3.

f

or

our

e

is

ted

|

Potassium ion (K⁺) channels have a modular structure with sensor domains connected to a central ion-conducting pore (1). The pore integrates signals coming from the sensors and translates them into opening or closing the channel (2). This allows K⁺ channels to alter the membrane potential of cells in response to a variety of physiological stimuli. Extending the range of signal inputs recognized by K⁺ channels can be achieved by grafting exogenous sensor domains onto the pore module (3, 4). With this modular interplay between sensor and pore, it is possible to engineer synthetic channels that respond to any signal by *ex novo* coupling of sensors to pores. This strategy provides new tools for the investigation and manipulation of biological functions (5). An attractive synthetic channel in this context is a light-gated K⁺ channel, which is important because of the ability of K⁺ to terminate excitatory currents within cells. This device would allow remote manipulation of the membrane potential with high temporal and spatial resolution and would represent an efficient control mechanism for many cellular processes, including neuronal firing and hormone release.

Several attempts have been made to create synthetic light-gated K⁺ channels (6–9); however, these systems suffer from several shortcomings in that they require the addition of cofactors (6, 7), are irreversible (8), or rely on multiple components (9). To overcome these obstacles, we engineered a single-component light-gated K⁺ channel by fusing the LOV2-J_α photosensory region of a plant blue-light receptor (10) to the miniature K⁺ channel pore Kcv (11). Rational design and di-

rected evolution were employed to ultimately generate a blue-light-inducible K⁺ channel that functions reversibly to drive cell membrane potentials to K⁺ equilibrium in the absence of exogenous cofactors. The LOV2-J_α photoswitch from *Avena sativa* phototropin 1 (hereafter LOV) can be used to control protein activity by light-induced conformational changes (12). We therefore adopted this strategy to place Kcv under light control. LOV was fused to various regions of Kcv known to be mechanically important for channel gating (fig. S1A and constructs 3 to 12 in table S1).

A functional complementation approach based on the growth rescue of *Δtrk1 Δtrk2* potassium transport-deficient yeast (strain SGY1528) (13) was adapted to screen for light-gated channel activity after replica plating (fig. S1B). One Kcv variant with LOV fused at the N terminus (LK) showed light-induced growth on selective agar (4 mM K⁺) and liquid culture (fig. S1, B and C). LK was expressed in *Xenopus* oocytes and tested by a two-electrode voltage clamp. LK currents showed modest but reproducible increases in conductance after transfer from darkness to blue light (455 nm, 80 μW/mm²) (fig. S2A). However, photostimulation of LK currents required tens of minutes to develop and appeared to be irreversible. In an attempt to enhance coupling of LOV to Kcv, the soluble photosensory region of LK was tethered to the plasma membrane. Introducing a putative myristoylation/palmitoylation sequence (MGCTVSAE) (14) at the N terminus of LK resulted in improved, but unexpected, properties. The new variant myLK (Fig. 1A and fig. S2B) showed an enhanced response to light compared with LK, but, in this case, light was found to inhibit rather than activate the channel conductance (fig. S2B). Moreover, the effect of light was reversible and it did not decrease after repetitive exposures. The light sensitivity of the channel was wavelength-specific, elicited by blue but not by red light (fig. S2B). The dynamic range of the light effect (DR), i.e., the ratio between light and dark current, was approximately 1.3. To improve the performance of myLK, three point

¹Department of Biosciences, University of Milano, Italy.

²Institute of Molecular, Cell and Systems Biology, University of Glasgow, UK. ³Department of Plant Pathology and Nebraska Center for Virology, University of Nebraska-Lincoln, Lincoln, NE 68583-0900, USA. ⁴Membrane Biophysics, Technical University of Darmstadt, Darmstadt, Germany.

*Present address: Illumina Italy, Via Senigallia 18/2, Milano 20161, Italy. †Corresponding author. E-mail: anna.moroni@unimi.it

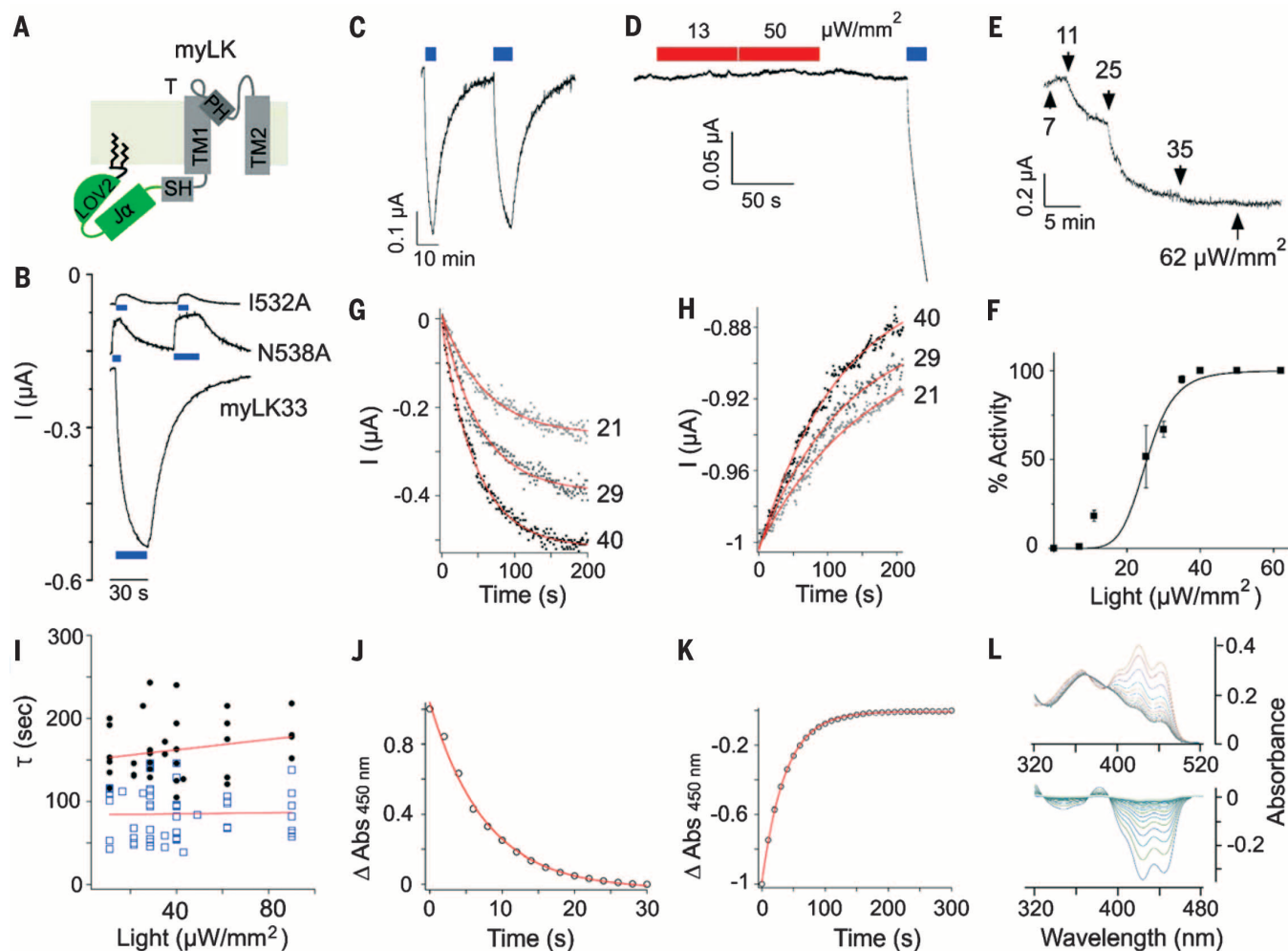


Fig. 1. Engineering and functional characterization of light-gated myLK channels. (A) Cartoon representation of myLK engineered by fusing LOV to Kcv with an additional N terminal myristoylation/palmitoylation sequence; myLK is shown as a monomer in the membrane. Kcv comprises slide helix (SH), pore-helix (PH), turret (T), and transmembrane domains (TM1 and TM2) (23). The LOV domain includes LOV2 and J α (10). Jagged lines indicate lipid anchoring to the membrane. (B) Currents recorded at -60 mV in 100 mM $[K^+]_{out}$ from oocytes expressing myLK mutants: I532A, N538A, and myLK33. Note that myLK I532A and N538A conductances are inhibited by blue light (blue bars, 455 nm), whereas that of myLK33 is activated. (C) Repetitive photoactivation of myLK33 shows the reproducibility of the effect. (D) Red light (red bars, 617 nm) at two light intensities, 13 and 50 $\mu\text{W}/\text{mm}^2$, does not activate myLK33 current, whereas blue light does. (E) Current response of myLK33 to increasing light intensities recorded at -80 mV showing threshold (>7 $\mu\text{W}/\text{mm}^2$) and saturating (35 $\mu\text{W}/\text{mm}^2$) values of light intensity. (F) Dose-response curve obtained from $n = 4$ oocytes. Line indicates data fitting by a Hill-type equation, yielding a dissociation constant $k = 25$ $\mu\text{W}/\text{mm}^2$ and a Hill coefficient $n = 6$. (G) Kinetics of myLK33 activation by different intensities of blue light and (H) subsequent inactivation in the dark. An oocyte expressing myLK33 was exposed to a re-

petitive light/dark regime with increasing light intensities ranging from low (21 $\mu\text{W}/\text{mm}^2$) to medium (29 $\mu\text{W}/\text{mm}^2$) to saturating (40 $\mu\text{W}/\text{mm}^2$) intensities. The current responses to the three light treatments are normalized to common starting values $I = 0$ for the onset of channel activation and $I = -1$ for the start of current decay in the dark; numbers on current traces indicate the light intensities in $\mu\text{W}/\text{mm}^2$. Fitting of data with single exponential equation (red lines) yields similar τ_{on} values for low (21 $\mu\text{W}/\text{mm}^2$, $\tau = 49$ s), medium (29 $\mu\text{W}/\text{mm}^2$, $\tau = 52$ s), and high (40 $\mu\text{W}/\text{mm}^2$, $\tau = 59$ s) light intensity. Currents decay in the dark with the same velocity, irrespective of pretreatment with a high ($\tau = 148$ s), medium ($\tau = 137$ s), or low ($\tau = 158$ s) light. (I) τ_{on} (blue symbols) and τ_{off} (black symbols) from a large number of independent experiments plotted as a function of light intensity. (J) Photoadduct formation kinetics for myL (construct 13, table S1) expressed and purified from *Escherichia coli*. Light-induced absorption changes were recorded at 450 nm ($\Delta\text{Abs}_{450 \text{ nm}}$) in response to blue-light irradiation (455 nm, 90 $\mu\text{W}/\text{mm}^2$) and show exponential kinetics ($\tau_{on} = 76$ s). (K) Dark recovery of $\text{Abs}_{450 \text{ nm}}$ after light excitation shows exponential kinetics ($\tau_{off} = 38$ s). (L) Representative light-induced absorption spectra of myL recorded at 2-s intervals (upper panel) and light-minus-dark difference spectra recorded every 10 s (lower panel).

mutations (G528A, I532A, and N538A) known to augment LOV-effector protein interactions (15) were introduced into the construct, singly or in combination (constructs 15 to 21, table S1). Several of these variants exhibited robust differential growth over a range of selective conditions (fig. S3). Notably, two mutants, myLK1532A and myLK1538A, had increased DR values, 1.5 and 1.9,

respectively (Fig. 1B), confirming that myLK architecture enables rational protein design.

To screen for additional DR improvements, random mutagenesis was performed using myLK538A to generate a library of myLK-encoding sequences. Potassium transport-deficient yeasts, transformed with this mutant library, were grown initially on nonselective

agar plates and then replica-plated onto selective medium before exposure to darkness or light. Yeast expressing the parental myLK538A channel did not grow on media with $[K^+]_{out}$ below 4 mM. Thus, variants growing below this concentration were selected for further characterization. Thirty-five variants were obtained showing strong differential growth in the light (either

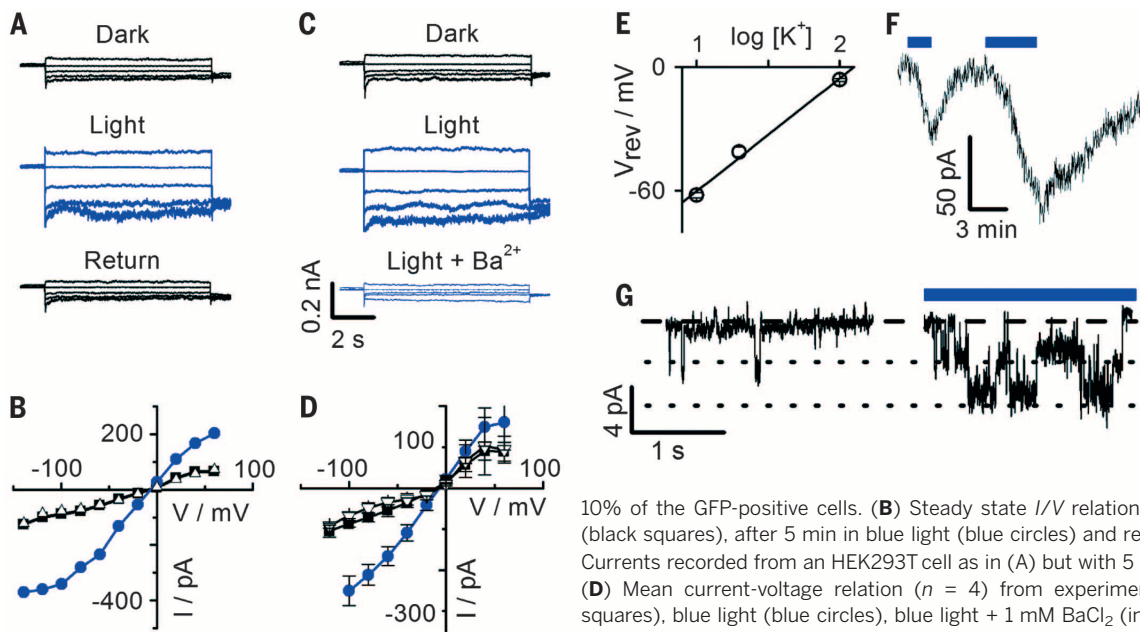


Fig. 2. Properties of BLINK1 in HEK293T cells. (A) Whole-cell currents recorded in HEK293T cells expressing myLJSK (BLINK1), in dark, blue light (455 nm, 40 $\mu\text{W}/\text{mm}^2$) and after returning to the dark. Voltage steps from +60 to -120 mV, tails at -80 mV (selected traces are shown every 40 mV). A measurable current, above the background, was found in about 8 to

10% of the GFP-positive cells. (B) Steady state I/V relation from currents in (A): dark (black squares), after 5 min in blue light (blue circles) and return in dark (triangles). (C) Currents recorded from an HEK293T cell as in (A) but with 5 mM of BaCl_2 added in light. (D) Mean current-voltage relation ($n = 4$) from experiments as in (B): dark (black squares), blue light (blue circles), blue light + 1 mM BaCl_2 (inverted triangles). (E) Mean V_{rev} values ($n = 3$) of light-activated BLINK1 current plotted as a function of $[\text{K}^+]_{\text{out}}$; slope = 58 mV/log $[\text{K}^+]$. Pipette solution contained 130 mM K^+ . (F) Repetitive activation/deactivation of BLINK1 current at -70 mV by blue light/dark transitions. (G) Single-channel fluctuations recorded at -70 mV from the same BLINK1-expressing cell in dark (left) and in blue light (right). Dashed line indicates zero current level; dotted lines indicate apparent single-channel opening levels. Calculated single-channel conductance is 70 pS.

activation or inhibition), 13 of which survived a second round of selection (to eliminate false positives) and were sequenced. The recovered mutations mapped throughout the randomized portion of myLK, but a subset clustered around proline 13 of Kcv (fig. S4), a residue known to affect channel gating (16). Notably, one particular variant, myLK33 (construct 33, fig. S4), harboring a mutation in P13 (P13L) and in the myristoylation/palmitoylation sequence (A7T), was activated rather than inhibited by light, with a relatively large DR value (DR = 3) (Fig. 1B). MyLK33 was therefore chosen for extensive functional characterization.

The channel could be repeatedly activated by light when expressed in oocytes without undergoing apparent inactivation (Fig. 1C). Activation was blue-light specific because red light had no perceivable effect on channel activity (Fig. 1D). By exposing the oocyte to increasing light intensities (Fig. 1E), we obtained a sigmoidal current response with a distinct activation threshold (Fig. 1F). The mean dose-response curve was best fitted with a Hill function yielding a value for half-activation, $k = 25 \mu\text{W}/\text{mm}^2$, and a Hill coefficient $n = 6$. This operational light sensitivity of the cell is less by a factor of about 500 than that of cells expressing light-sensitive pumps such as NpHR (17).

To obtain information on the kinetics of channel activation/deactivation in light/dark, cells were irradiated with different intensities of blue light and transferred back into darkness. Activation and deactivation kinetics could be fitted with a single exponential function (Fig. 1, G and H). The time constants did not change over a wide range of light intensities, from suboptimal to saturating (Fig. 1I). Activation (τ_{on} , 87 ± 28 s, $n = 52$) was

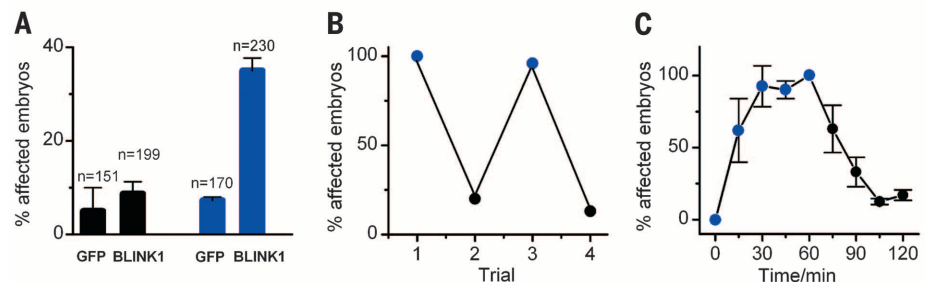


Fig. 3. Light controls the behavior of zebrafish expressing BLINK1. (A) Altered escape response in 2-day-old zebrafish, expressing BLINK1 or GFP. The embryos were injected at t_0 , kept 24 hours in the dark, and then either exposed to blue light (80 $\mu\text{W}/\text{mm}^2$) (blue) or kept in the dark (black). The escape response was tested by gentle mechanical stimulation with a pipette tip (see movie S1). Number of embryos (n) is indicated. (B) Reversibility of the effect of blue light on the escape response. Each data point represents the response of a batch of 2-day-old BLINK1-injected embryos, preselected for positive light response ($n = 15$). The embryos were repetitively exposed to blue light (blue circles) and dark (black circles) treatments (30 to 45 min each). (C) Kinetics of the light effect on the escape response of 2-day-old embryos. At time zero, blue light was turned on and the response to mechanical stimulation was checked every 15 min. After 60 min, the effect reached the maximum and the light was turned off to monitor the deactivation kinetics. Data are from three experiments in which the n of responding embryos was 62 over a total number of 163 (38%). Data were normalized to the maximum number of responding embryos at plateau in each experiment (after 60 min of light).

about twice as fast as deactivation (τ_{off} 168 ± 31 s, $n = 43$). To further examine the relationship between channel gating and the photocycle of the sensor, we performed spectroscopic measurements on the sensor portion of the protein (myL), which was used to construct the channel. Global photoadduct formation at saturating light intensity (90 $\mu\text{W}/\text{mm}^2$) and its recovery in the dark (Fig. 1, J to L) show exponential kinetics with values of 7.6 s for τ_{on} and 38 s for τ_{off} . Hence, myL activates, under the same light conditions, about 10 times as fast as the channel, whereas photo-

adduct decay is about 4.5 times as fast as channel deactivation in the dark. Thus, the primary light sensing by the photosensor seems to be only loosely correlated with channel gating. This agrees with the observation that other constructs harboring the same photoswitch as myLK33 (see, for example, I532A and N538A) responded to light with a different kinetics (Fig. 1B). Together, these findings suggest that light-regulated channel activity is mostly dominated by slow conformational changes that follow LOV2-*Ja* photo activation.

Experimental evidence that myLK33 retains the pore properties of the parental K⁺-selective channel Kcv is summarized in fig. S5. Barium, a known Kcv channel blocker, completely inhibited both dark- and light-induced currents of myLK33 (fig. S5A). The current-voltage (*I-V*) curve (fig. S5B) shows that light activation of myLK33 is voltage-independent. The reversal potentials (V_{rev}) of myLK33 photocurrent shifted according to the Nernst equation by 51 mV for a 10-fold increase in external K⁺ concentration, a value similar to that of Kcv (*I*) (fig. S5C). Moreover, exchanging 100 mM external K⁺ with Na⁺ shifted V_{rev} to the left by 110 mV, indicating a very low Na⁺ permeability ($P_{Na}/P_K = 0.015 \pm 0.001$ ($n = 4$) (fig. S5D).

Despite these desirable features, *in vivo* application of myLK33 is hampered by its high dark activity. We have previously shown in other synthetic channels that the linker between the sensor and the effector module influences the coupling of the two (4). We therefore progressively reduced the linker region within myLK in an attempt to improve the control of the photosensor over the channel pore (constructs 23 to 37 in table S1 and fig. S6). Best results were obtained with myLJSK, which lacks the final nine amino acid residues within the J α helix (fig. S7A). This variant showed stringent differential growth in the yeast complementation assay (fig. S7B) but was poorly expressed in oocytes. Immunolabeling showed that this channel is present on the membrane of human embryonic kidney 293T (HEK293T) cells, albeit at a moderate level, when compared with the parental channel Kcv (fig. S7C). Subsequent electrophysiological characterization in HEK293T cells demonstrated that myLJSK is activated by blue light (Fig. 2, A and B). Light activation is fully reversible in the dark (Fig. 2, A and B) and inhibited by Ba²⁺ (Fig. 2, C and D). Importantly, myLJSK lacks any channel activity in darkness, as evident from the comparison of the amount of current in the dark and in the presence of Ba²⁺ (fig. S7D). Channel opening moves the reversal potential of the cell with E_K , the K⁺ equilibrium voltage (Fig. 2E). The light sensitivity of myLJSK occurs in the same range as that of myLK33, being saturated at $\sim 60 \mu\text{W}/\text{mm}^2$ (fig. S7E).

Light gating of myLJSK is best appreciated in gap-free recordings. Repetitive exposure to blue light caused rapid activation followed by deactivation in darkness (Fig. 2F). Data recorded from single-channel fluctuations (Fig. 2G) showed a light-induced increase in channel activity and indicated a unitary conductance of about 70 pS, consistent with the high conductance of Kcv and its synthetic variant Kv_{Synth1} (4). The high single-channel conductance and the relatively low macroscopic currents (≤ 400 pA at -100 mV) are consistent with the low number of channels, which were detectable by immunolocalization (fig. S7C). A low number of channel proteins with a large unitary conductance offers the advantage of an efficient control over the membrane voltage with minimal disturbance of the cell. These properties of myLJSK ultimately fulfilled our criteria for successful light gating of Kcv. Hence, we re-

named this variant BLINK1, blue-light-induced K⁺ channel 1. Expression of BLINK1 in Sf9 insect cells (fig. S8A) produced fluorescence properties that are characteristic for LOV-containing proteins (fig. S8, B and C). Photoadduct formation and decay for BLINK1 was therefore analyzed by fluorescence spectroscopy and showed kinetics similar to those obtained for myLOV *in vitro* (14.5 s for τ_{on} and 51s for τ_{off}) (fig. S8, D and E).

To determine the *in vivo* applicability of BLINK1 for optogenetics, we examined its ability to regulate the escape response of zebrafish embryos. Two-day old embryos respond to touch with a burst of swimming (18). We reasoned that BLINK1 photoactivation in zebrafish neurons (either somatosensory or motor) and/or in myocytes would prevent or drastically impair this behavior. Embryos injected with either BLINK1 or green fluorescent protein (GFP) RNA showed robust escape motions when kept in darkness [over 90% of embryos in both cases (BLINK1, $n = 199$; GFP, $n = 151$)]. By contrast, when embryos were exposed to blue light, 37% of BLINK1-expressing embryos exhibited a reduced escape response ($n = 230$) compared with just 9% in control larvae ($n = 170$) (Fig. 3A and movie S1). The blue-light effect was fully and repetitively reverted in darkness (Fig. 3B), as expected for a BLINK1-driven effect. The light-driven effect on embryonic escape motion developed with a half-time of 15 to 20 min and was reverted by dark with a similar kinetics (Fig. 3C).

Several additional observations underscored that BLINK1 was expressed in zebrafish and that altered behavior of the larvae was driven directly by its activation in blue light. First, the presence of the channel is detectable by Western blotting in BLINK1-injected embryos (fig. S9A). Second, the success of eliciting escape behavior was highly dependent on the wavelength of light with red light (617 nm) being ineffective at evoking altered behavior (fig. S9B). Third, in the dark, viability and morphology were similar in embryos expressing BLINK1 or GFP (wild-type embryos at 2dpf BLINK1 = 77%, $n = 81$; GFP = 69%, $n = 59$), confirming that BLINK1 is tightly closed in the absence of light. Taken together, these data demonstrate the ability of BLINK1 to modulate behavioral responses *in vivo*.

In conclusion, we have created a light-activated K⁺ selective channel by combining a blue-light sensor and a simple K⁺ channel pore. The resulting BLINK1 channel is fully genetically encoded and does not depend on external factors for its light regulation, as the flavin mononucleotide chromophore is ubiquitously present in cells. BLINK1 is therefore a promising tool in optogenetics and has several desirable properties relative to other light-gated pumps (17, 19, 20) and channels (21, 22) used for inhibiting the functions of excitable cells. First, in contrast to light-gated pumps, which move H⁺ or Cl⁻ ions, it moves K⁺, a physiological ion, down its electrochemical equilibrium. Thus, BLINK1 does not expose the cell to unphysiological hyperpolarizations or ion gradients. Second, its large unitary conductance guarantees that a small number of channels can

efficiently decrease the input resistance of cells and hyperpolarize the membrane. In addition, the channel does not inactivate in light, which allows long-term control of channel activity by light. The apparent sensitivity of BLINK1 to light, combined with its slow kinetics, makes it a powerful tool for long-term inhibition of cells at low light intensities. Our pilot experiments in zebrafish demonstrate that BLINK1 can be successfully used as an *in vivo* optogenetic tool. Besides an obvious application for inhibiting neuronal activity, this channel will also find applications in the control of cellular processes, which require long-term stabilization of the membrane voltage such as cell cycle regulation or the control of hormone secretion.

REFERENCES AND NOTES

- S. B. Long, E. B. Campbell, R. Mackinnon, *Science* **309**, 897–903 (2005).
- R. Latorre, F. J. Morera, C. Zaelzer, *J. Physiol.* **588**, 3141–3148 (2010).
- U. M. Ohndorf, R. MacKinnon, *J. Mol. Biol.* **350**, 857–865 (2005).
- C. Arrigoni et al., *J. Gen. Physiol.* **141**, 389–395 (2013).
- M. R. Banghart, M. Volgraf, D. Trauner, *Biochemistry* **45**, 15129–15141 (2006).
- M. Banghart, K. Borges, E. Isacoff, D. Trauner, R. H. Kramer, *Nat. Neurosci.* **7**, 1381–1386 (2004).
- H. Janovjak, S. Szobota, C. Wyart, D. Trauner, E. Y. Isacoff, *Nat. Neurosci.* **13**, 1027–1032 (2010).
- J. Y. Kang et al., *Neuron* **80**, 358–370 (2013).
- D. Schmidt, P. W. Tillberg, F. Chen, E. S. Boyden, *Nat. Commun.* **5**, 3019 (2014).
- J. M. Christie, *Annu. Rev. Plant Biol.* **58**, 21–45 (2007).
- B. Plugge et al., *Science* **287**, 1641–1644 (2000).
- J. M. Christie, J. Gawthorne, G. Young, N. J. Fraser, A. J. Roe, *Mol. Plant* **5**, 533–544 (2012).
- F. C. Chatelain et al., *PLOS ONE* **4**, e7496 (2009).
- C. Aicart-Ramos, R. A. Valero, I. Rodriguez-Crespo, *Biochim. Biophys. Acta* **1808**, 2981–2994 (2011).
- D. Strickland et al., *Nat. Methods* **7**, 623–626 (2010).
- B. Hertel et al., *Eur. Biophys. J.* **39**, 1057–1068 (2010).
- J. Mattis et al., *Nat. Methods* **9**, 159–172 (2011).
- R. M. Colwill, R. Creton, *Rev. Neurosci.* **22**, 63–73 (2011).
- F. Zhang et al., *Nature* **446**, 633–639 (2007).
- X. Han, E. S. Boyden, *PLOS ONE* **2**, e299 (2007).
- A. Berndt, S. Y. Lee, C. Ramakrishnan, K. Deisseroth, *Science* **344**, 420–424 (2014).
- J. Wietek et al., *Science* **344**, 409–412 (2014).
- S. S. Tayfeh et al., *Biophys. J.* **96**, 485–498 (2009).

ACKNOWLEDGMENTS

We thank G. Romani for providing the antibody to Kcv; D. Minor for the *Saccharomyces cerevisiae* SGY1528 strain; U. P. Hansen, I. Schroeder, and A. Bertl for helpful discussion; and M. Ascagni for technical help with confocal microscopy. This work was supported by Fondazione Cariplo grant 2009-3519, PRIN (Programmi di Ricerca di Rilevante Interesse Nazionale) 2010CSJX4F, and MAE (Ministero Affari Esteri) 01467532013-06-27 to A.M.; by the UK Biotechnology and Biological Sciences Research Council (BB/J016047/1 and BB/M002128) to J.M.C.; and by the Landes-Offensive zur Entwicklung Wissenschaftlich-ökonomischer Exzellenz (LOEWE) initiative Soft Control to G.T.

SUPPLEMENTARY MATERIALS

www.sciencemag.org/content/348/6235/707/suppl/DC1

Materials and Methods

Figs. S1 to S9

Table S1

Movie S1

References (24–31)

11 November 2014; accepted 7 April 2015

10.1126/science.aaa2787

Engineering of a light-gated potassium channel

Cristian Cosentino, Laura Alberio, Sabrina Gazzarrini, Marco Aquila, Edoardo Romano, Solei Cermenati, Paolo Zuccolini, Jan Petersen, Monica Beltrame, James L. Van Etten, John M. Christie, Gerhard Thiel and Anna Moroni

Science **348** (6235), 707-710.
DOI: 10.1126/science.aaa2787

An optogenetic tool to silence neurons

Potassium channels in the cell membrane open and close in response to molecular signals to alter the local membrane potential. Cosentino *et al.* linked a light-responsive module to the pore of a potassium channel to build a genetically encoded channel called BLINK1 that is closed in the dark and opens in response to low doses of blue light. Zebrafish embryos expressing BLINK1 in their neurons changed their behavior in response to blue light.

Science, this issue p. 707

ARTICLE TOOLS

<http://science.sciencemag.org/content/348/6235/707>

SUPPLEMENTARY MATERIALS

<http://science.sciencemag.org/content/suppl/2015/05/06/348.6235.707.DC1>

RELATED CONTENT

<http://stke.sciencemag.org/content/sigtrans/7/319/re1.full>
<http://stm.sciencemag.org/content/scitransmed/5/177/177ps5.full>
<http://stm.sciencemag.org/content/scitransmed/5/177/177ps6.full>

REFERENCES

This article cites 31 articles, 9 of which you can access for free
<http://science.sciencemag.org/content/348/6235/707#BIBL>

PERMISSIONS

<http://www.sciencemag.org/help/reprints-and-permissions>

Supplementary Materials for

Engineering of a light-gated potassium channel

Cristian Cosentino, Laura Alberio, Sabrina Gazzarrini, Marco Aquila, Edoardo Romano, Solei Cermenati, Paolo Zuccolini, Jan Petersen, Monica Beltrame, James L. Van Etten, John M. Christie, Gerhard Thiel, Anna Moroni*

*Corresponding author. E-mail: anna.moroni@unimi.it

Published 8 May 2015, *Science* **348**, 707 (2015)
DOI: [10.1126/science.aaa2787](https://doi.org/10.1126/science.aaa2787)

This PDF file includes:

Materials and Methods
Figs. S1 to S9
Table S1
References

Other Supplementary Material for this manuscript includes the following:
(available at www.sciencemag.org/cgi/content/full/348/6235/707/DC1)

Movie S1

Supplementary Materials for

Engineering of a light-gated potassium channel

Cristian Cosentino, Laura Alberio, Sabrina Gazzarrini, Marco Aquila, Edoardo Romano, Solei Cermenati, Paolo Zuccolini, Jan Petersen, Monica Beltrame, James L. Van Etten, John M. Christie, Gerhard Thiel and Anna Moroni

This section includes:

Materials and Methods

Figures S1-S9

Tables S1

Movie S1

Supplementary References

Materials and Methods:

Cloning procedures and plasmids

All constructs were prepared by adding the LOV2 domain, aa 404-546 of *Avena sativa* Phototropin 1 (NPH1-1 GenBank: AAC05083.1) (24) to Kcv, aa 2-94 of chlorovirus PBCV-1-Kcv (NP_048599.1) (11) by overlapping PCR. The complete list of mutations, deletions and insertions, which were introduced in each construct, is reported in Table S1. Mutations introduced either in the LOV domain or in Kcv are numbered on the original sequences of phototropin and Kcv. Overlapping PCR was used to add the N-terminal myristoylation and palmitoylation sequence (MGCTVSAE) (14) to the N terminus of the construct and QuikChange XL II (Agilent Technologies) was used to introduce point mutations. Coding sequences were cloned in pYES2-Met25 vector (25) for *S.*

cerevisiae expression; in pSGEM (a modified version of pGEM-HE vector) for expression in *Xenopus laevis* oocytes; in pCDNA3.1+ for HEK293T cells expression; in a modified version of pET-21d containing a 7His-Strep II-SUMO tag (26) for expression in *E. coli* and in pCS2+ for zebrafish expression. The plasmid for expression in SF9 *Spodoptera frugiperda* cells was built by Gibson assembly (27) using pAcHLT-A digested with *SphI* and *SacI* as backbone, a fragment amplified from pAcHLT-A (base pairs 215-2203) and the BLINK1 coding sequence amplified with a 3' primer creating a C-terminal 6His-tag.

Yeast functional complementation assays

Functional complementation assays were performed using the *S. cerevisiae* strain SGY1528 (*MATa ade2-1 can1-100 his3-11,15 leu2-3,112 trp1-1 ura3-1 trk1::HIS3 trk2::TRP1* (25, 28) This strain lacks the endogenous K⁺ uptake system and it is not able to grow on media supplemented with K⁺ lower than 100 mM.

To test the functionality of the clones, yeast colonies were inoculated in non-selective medium (SD - Ura, 100 mM KCl) and grown overnight to stationary phase. Cultures were then diluted to OD₆₀₀ = 0.8 and 10-fold serial dilutions were spotted (7µl) onto selective plates (SEL -Ura -Met with 0.5, 1, 4 mM KCl). Twin plates were prepared for each K⁺ concentration and were either exposed to blue light or grown in the dark. After 3 and 4 days at 30°C images were taken and plates were screened for colonies with differential growth between Blue light and dark in the presence of low KCl concentration. To confirm functional complementation, cultures from overnight stationary phase were also inoculated in liquid selective media (SEL -Ura -Met with 4, 7, 10, 100 mM KCl) and grown for up to 117 h in presence of blue light or in the dark. OD₆₀₀ of the cultures were measured to determine the growth ratio between the two conditions at 21, 45, 52 and 117 h after inducing protein expression. Positive clones were selected for plasmid isolation and DNA amplification in *E. coli* for sequencing. Non-selective and selective media were prepared as previously described (25). Solid media were obtained adding 15g/l agar.

Yeast random library screening

Randomization was performed on the sequence coding the myristoylation and palmitoylation domain, the whole LOV domain and the Kcv channel up to the first transmembrane region, where the channel DNA sequence has an endogenous *SmaI* restriction site. Random mutagenized libraries were generated using the Gene Morph II random mutagenesis kit (Agilent Technologies) in three steps: two samples with 50 ng of myLK N538A were amplified by PCR (30 cycles) with PAGE-purified 60-mer primers (IDT-Tema Ricerca). The forward primer is complementary to the upstream plasmid sequence while the reverse primer is complementary to the Kcv sequence downstream of the *SmaI* restriction site (corresponding to the first transmembrane region). Two μl of each PCR reaction were used as template for a subsequent amplification reaction (30 cycles). This was repeated twice. The end products of the final six reactions were gel-purified, grouped and gap-repaired in yeast SGY1528 strain with *SmaI* linearized pYES2-Met25 plasmid containing wild-type myLK N538A. Co-transformation was performed with a Frozen-EZ yeast transformation II kit (Zymo Research). The library was first plated on non-selective medium (SD –Ura with 100 mM KCl) and grown for 3 days at 30 °C, in dark, yielding roughly 20000 transformed colonies. Non-selective plates were then replica-plated twice onto selective plates (SEL –Ura -Met with 0.5 mM KCl) and grown for 3 days at 30 °C under blue light or dark conditions. Colonies showing differential growth between the two conditions were selected for subsequent functional complementation assays.

Electrophysiology

Xenopus oocytes - cRNAs were transcribed in vitro using T7 RNA polymerase (Promega) as described (11). Oocytes were prepared according to standard methods and injected with 50 nl of water or 50 nl of cRNA (0.8 $\mu\text{g}/\mu\text{l}$) and incubated in the dark at 19°C in ND96 solution : 96 mM NaCl, 2 mM KCl, 1.8 mM CaCl₂, 1mM MgCl₂, 5 mM HEPES–NaOH buffer (pH 7.5), 5 mM sodium pyruvate, 50 $\mu\text{g}/\text{ml}$ gentamicin). Measurements were performed 2-5 days after injection. Currents

were recorded by two-electrode voltage clamp, using the Gene-Clamp 500 amplifier (Axon Instruments) under control of pCLAMP7. Oocytes were perfused at room temperature with a solution containing: 100 mM KCl, 1.8 mM CaCl₂, 1 mM MgCl₂, and 5 mM HEPES-KOH buffer (pH 7.4). When different KCl concentrations were used, the osmolarity was adjusted to 215 mOsm with mannitol. The voltage protocols applied consisted in a step protocol of 20 mV steps from +60 to -180 mV or in a gap free protocol at -60 or -80 mV. The channel blocker BaCl₂ was applied to the external solution at a concentration of 1 or 5 mM, as indicated.

HEK293T cells - HEK293T cells were cultured in Dulbecco's modified Eagle's medium (Euroclone) supplemented with 10% fetal bovine serum (Euroclone), 100 IU/mL of penicillin and 100 µg/ml of streptomycin, and stored in a 37 °C humidified incubator with 5% CO₂. BLINK1 and myLK33 cDNAs were co-transfected in HEK293T with a plasmid containing green fluorescent protein (GFP). Transfections were performed with TurboFect Transfection Reagent (Thermo Scientific). One to two days after transfection, HEK293T cells were dispersed by trypsin treatment and placed on 35-mm plastic petri dishes. Cells showing a clear fluorescence signal were selected for patch clamp analysis. Membrane currents were recorded in whole cell configuration using a Dagan 3900A patch-clamp amplifier and digitized using a Digidata 1322A controlled by pCLAMP 9.2. The pipette solution contained: 10 mM NaCl, 130 mM KCl, 2 mM MgCl₂, and 5 mM HEPES-KOH buffer (pH 7.2). The extracellular bath's solution contained: 100 mM KCl, 80 mM D-Mannitol, 1.8 mM CaCl₂, 1 mM MgCl₂ and 5 mM HEPES-KOH buffer (pH 7.4). When different KCl concentrations were used, the osmolarity was adjusted to 290 mOsm with mannitol. The channel blocker BaCl₂ was applied to the external solution at a concentration of 1 or 5 mM.

Light stimulation

Yeast functional complementation assays were performed by means of a custom-made array of light emitting diodes (LEDs) (Royal-Blue LED, λ 447 ± 10 nm, LUXEON Rebel LED) for homogeneous

illumination of the samples ($2 \pm 0.2 \mu\text{W}/\text{mm}^2$) in a controlled temperature chamber. The same system was used for illumination of zebrafish embryos at $80 \mu\text{W}/\text{mm}^2$. Red light was also provided at $80 \mu\text{W}/\text{mm}^2$ by means of Red-Orange LED, λ 617 nm (MR-H2060-20T, LUXEON Rebel LEDs). Transfected HEK293T cells and injected oocytes were protected from ambient light to prevent receptor activation prior to the assays and all manipulations were performed under red light (MR-H2060-20T, LUXEON Rebel LEDs Red-Orange (617 nm)) in the Faraday cage shielded with a 580 nm cutoff filter (Rosco Supergel, Deep Amber #22). Blue light was provided by a light-emitting diode (Royal Blue, 455 nm, High-Power LED; Thorlabs) at intensity indicated in figure legends. Light power was measured using a handheld light power meter (Thorlabs).

Protein expression and spectroscopic analysis

For protein expression and purification, *E. coli* RosettaBL21(DE3)pLysS (Novagen) cells were grown in LB medium to an OD_{600} of 0.6, induced with 0.5 mM IPTG and incubated overnight at 24 °C. Cells were harvested and tandem affinity purified with subsequent SUMO protease cleavage of the tag as described (26).

Sf9 insect cells were grown in a monolayer with TC100 medium containing 10% FBS at 27 °C. For the construction of recombinant virus the transfer vector was co-transfected into cells with linearized baculovirus DNA using the BacMagic DNA Kit (Novagen). Transfected cells were incubated for 5 days to raise the primary viral stock. Two additional rounds of virus propagation (each for 3 days) were performed. High titer virus was used for protein expression. Cells were incubated in medium supplemented with 20 μM riboflavin for 3 days in darkness prior to harvest. For fluorescence emission and excitation measurements, the cells were washed to remove residual riboflavin and resuspended in Dulbecco's PBS at a density of 1.5×10^7 cells/ml.

Absorption spectra of purified protein from *E. coli* were collected with a Shimadzu MultiSpec-1501 diode array spectrophotometer at room temperature. *In vivo* fluorescence emission and excitation spectra of insect cells were recorded using a Perkin-Elmer LS-55 luminescence spectrometer. Fluorescence excitation spectra were recorded by monitoring the emission at 520 nm. Fluorescence emission spectra were obtained using an excitation wavelength of 450 nm. For absorbance and fluorescence measurements, a blue-light emitting diode (λ 455 nm) provided the excitation pulse.

Immunocytochemistry

HEK293T cells transfected with BLINK1 and Kcv-GFP (29) channels were treated with blocking solution containing 2% BSA in PBS. Cells were incubated 1 hour with anti-Kcv monoclonal antibody (30) washed briefly with blocking solution and incubated 1 hour with Alexa Fluor® 594 AffiniPure secondary antibody and Hoechst dye. Confocal microscopy analyses were performed using Leica SP2 (<http://www.leica-microsystems.com>) laser scanning confocal imaging system.

Microinjections and touch response assays in zebrafish

pCS2+BLINK1 and pCS2+GFP constructs were linearized with *NotI* and transcribed with Sp6 RNA polymerase, using the mMMESSAGE mMACHINE® SP6 Transcription Kit (Ambion) and following manufacturer's instructions. Embryos were injected at the 1- to 2-cell stage with 200pg/embryo of RNA in water (W3500, Sigma-Aldrich), supplemented with rhodamine-dextran (D1817, Molecular Probes) as a tracer. Injected embryos were raised in E3 medium (5 mM NaCl, 0.17 mM KCl, 0.33 mM MgSO₄, 0.33 mM CaCl₂) at 28.5 °C and manually dechorionated at 1 day post-fertilization (1 dpf). The screening for touch-evoked escape response was performed at 2 days post-fertilization (unless differently specified), following standardized procedures. Using a hand-broken microloader tip, a gentle stimulus was applied to the tail of the embryos and their reaction observed. Wild-type embryos at this developmental stage swim away from the source of the stimulus (31).

Western blot

Yeast microsome preparation-Yeast cells grown in liquid culture in selective medium for 3 days at 30 °C were pelleted (1,500 x g, 20 min). Pellet was resuspended in Breaking Buffer (50 mM NaH₂PO₄*H₂O, 1 mM EDTA, 5 % (w/v) glycerol, 5µM Leupeptin, 1µM Pepstatin, 0.1mM PMSF, 5mM DTT). Cells were broken by vortexing with glass beads (425-600 µm, Sigma-Aldrich) and centrifugated (4000 x g, 5 min) to remove cell debris. Then, the Eppendorf tube was centrifuged (15,000 x g, 1 hour) at 4°C and the supernatant was discarded. The microsomes were resuspended in Breaking Buffer and stored at -80 °C.

Preparation of zebrafish lysates- Deyolked embryos were resuspended in modified RIPA buffer (50mM Tris, 150mM KCl, 0.1%SDS, 5%DOC, 0.1% NP-40, filter sterilized) and homogenized using IKA T10 basic homogenizer. Lysates were quantified and stored at -80°C.

Insect cell protein extract - Cells were harvested (1,000 x g, 1min) and resuspended in Dulbecco's phosphate buffered saline supplemented with cOmplete EDTA-free protease inhibitor (Roche). Lysis of cells was performed by sonication with subsequent centrifugation (14,000 x g, 5 min) to remove cell debris.

Western blot analysis- 60 µg (zebrafish) or 13µg (yeast) /lane of total protein were separated on 4-20% tris-glycine denaturing gel (Novex). Proteins were blotted on a PVDF membrane and blots were blocked in 5% dry milk in TBST solution for 2 hours and incubated with primary anti-Kcv monoclonal antibody (30) at 4 °C overnight. Then the blots were rinsed in TBST for 3 X 10 min and incubated with alkaline phosphatase-conjugated secondary antibody for 1 hour. Antibody binding was detected using SIGMAFAST BCIP/NBT tablet (Sigma).

For immunodetection of BLINK1 protein expressed in insect cells, 20 µg of total protein were separated by SDS-PAGE on a 4-20% gradient gel (BioRad) and transferred to a nitrocellulose membrane. The membrane was blocked for 1 h with TBST containing 4% milk powder, followed by 1 h incubation with the first antibody (anti-Kcv). Afterwards the membrane was washed 3 x TBST

for 10 min each, incubated with the secondary HRP conjugated antibody for 45 min and then washed again as described before. Detection of immune complexes was made with ECL (Pierce) according to manufacturer's instructions and a Fusion Fx imager (peqlab) used to record the signal.

Table S1. List of constructs and details on their sequences. L= LOV domain (LOV2 and J α); K= Kcv; my= myristoylation and palmytoylation sequence MGCTVSAE; GIN= mutations G528A, I532A and N538A (NPH1.1 numbering); M = methionine residue inserted N terminal to L. All constructs have been functionally characterized in yeast or/and in oocytes.

	NR	NAME	DETAILS
CONTROLS	1	Kcv	Kcv PBCV-1 (1-94)
	2	L	AsPhotI (404-546) NPH1.1, GenBank: AAC05083.1
LOV COUPLING TO KCV	3	KL	PBCV-1 (1-94) ::LOV2 (404-546)
	4	KIdL	PBCV-1 (1-94) ::D ::LOV2 (404-546)
	5	KPPL	PBCV-1 (1-32) ::LOV2 (404-546) ::PBCV-1 (44-94)
	6	KGGL	PBCV-1 (1-34) ::LOV2 (404-546) ::PBCV-1 (33-94)
	7	KLK	PBCV-1 (1-94) ::LOV2 (404-546) ::PBCV-1 (3-94)
	8	LK	M ::LOV2 (404-546) ::PBCV-1 (3-94)
	9	LK S Δ 2	M ::LOV2 (404-544) ::PBCV-1 (3-94)
	10	LK S Δ 6	M ::LOV2 (404-544) ::PBCV-1 (7-94)
	11	LK S Δ 10	M ::LOV2 (404-544) ::PBCV-1 (11-94)
	12	LSK	M ::LOV2 (404-522) ::PBCV-1 (3-94)
my CONTROLS	13	myL	my(1-8) ::LOV2 (404-546)
	14	myLK	my(1-8) ::LOV2 (404-546) ::PBCV-1 (3-94)
RATIONAL MUTAGENESIS	15	myLK I	my(1-8) ::LOV2 (404-546) I532A ::PBCV-1 (3-94)
	16	myLK G	my(1-8) ::LOV2 (404-546) G528A ::PBCV-1 (3-94)
	17	myLK N	my(1-8) ::LOV2 (404-546) N538A/E ::PBCV-1 (3-94)
	18	myLK GN	my(1-8) ::LOV2 (404-546) G528A N538A/E ::PBCV-1 (3-94)
	19	myLK IN	my(1-8) ::LOV2 (404-546) I532A N538A ::PBCV-1 (3-94)
	20	myLK GI	my(1-8) ::LOV2 (404-546) G528A I532A ::PBCV-1 (3-94)
	21	myLK GIN	my(1-8) ::LOV2 (404-546) G528A I532A N538A ::PBCV-1 (3-94)
RANDOM MUTAGENESIS	22	myLK33	my(1-8) A7T ::LOV2 (404-546) N538A ::PBCV-1 (3-94) P13L
LINKER MODIFICATIONS	23	myLK33 Δ 6	my(1-8) A7T ::LOV2 (404-546) N538A ::PBCV-1 (9-94) P13L
	24	myLK33 Δ 9	my(1-8) A7T ::LOV2 (404-543) N538A ::PBCV-1 (9-94) P13L
	25	myLK33 Δ 28	my(1-8) A7T ::LOV2 (404-522) N538A ::PBCV-1 (7-94) P13L
	26	myLK33 Δ (KEL)	my(1-8) A7T ::LOV2 (404-543) N538A ::PBCV-1 (3-94) P13L
	27	myLK Δ 9	my(1-8) ::LOV2 (404-541) ::PBCV-1 (7-94)
	28	myLSK	my(1-8) ::LOV2 (404-522) ::PBCV-1 (3-94)
	29	myLJ21SK	my(1-8) ::LOV2 (404-543) ::PBCV-1 (6-94)
	30	myLJ18SK	my(1-8) ::LOV2 (404-540) ::PBCV-1 (6-94)
	31	myLTKdp	my(1-8) ::LOV2 (404-522) ::PBCV-1 (13-94)
	32	myLTKep	my(1-8) ::LOV2 (404-517) ::PBCV-1 (12-94)
	33	myLTKdr	my(1-8) ::LOV2 (404-522) ::PBCV-1 (10-94)
	34	myLJK	my(1-8) ::LOV2 (404-544) ::PBCV-1 (11-94)
	35	myLJSK	my(1-8) ::LOV2 (404-537) ::PBCV-1 (3-94)
	36	myLK Δ (KEL)	my(1-8) ::LOV2 (404-543) ::PBCV-1 (3-94)
	37	myLK N Δ (KEL)	my(1-8) ::LOV2 (404-543) N538A ::PBCV-1 (3-94)

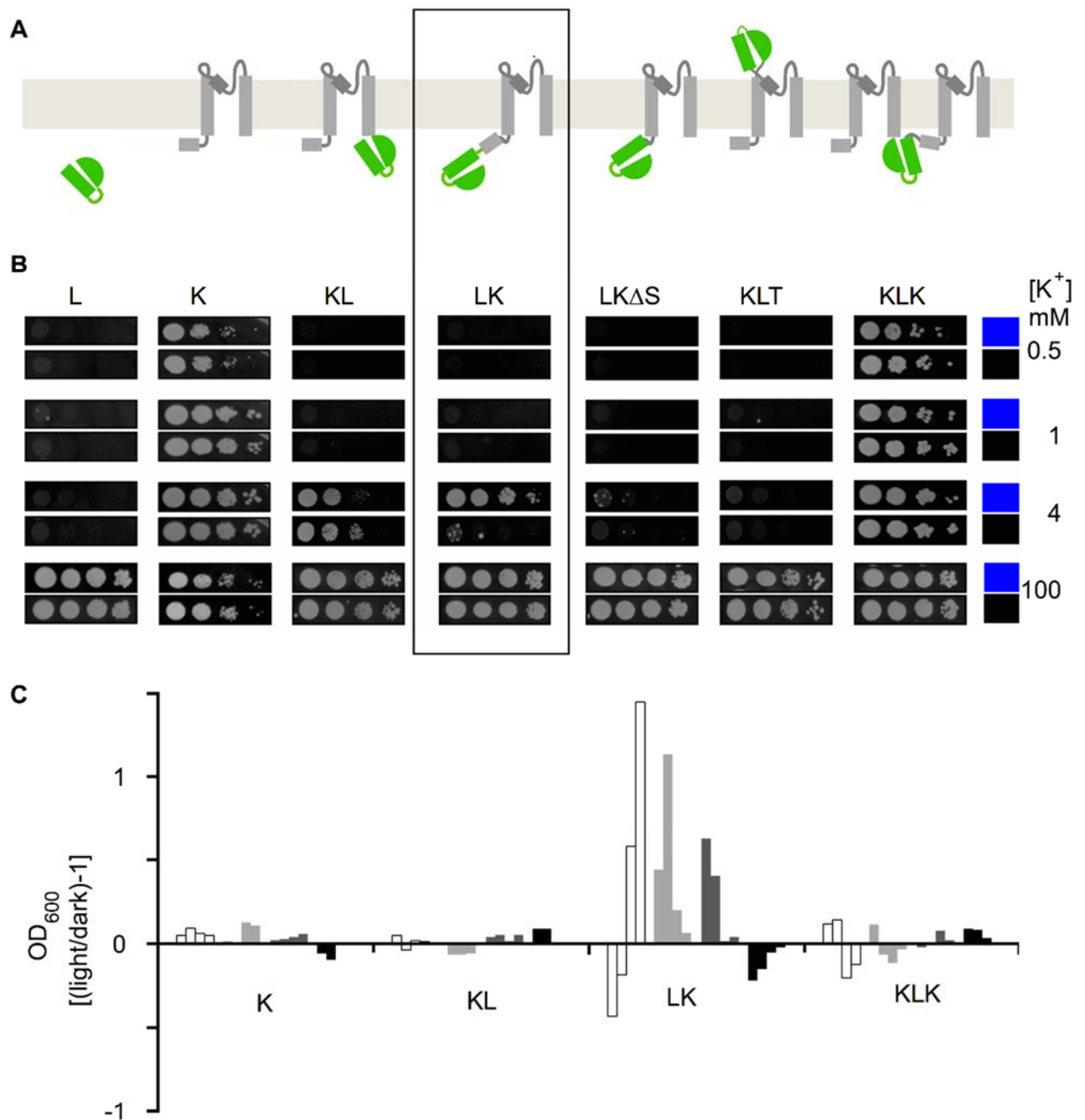


Figure S1. Steps to developing rudimental light sensitivity in the K^+ channel Kcv

(A) Cartoon representation of the constructs engineered by fusing the light sensor to several positions. LOV domain is in green; Kcv in grey. The constructs are shown as monomers inserted into the lipid bilayer. (B) Functional complementation of $\Delta trk1 \Delta trk2$ potassium transport deficient growth in solid medium with the above constructs named as follow: L, LOV domain; K, Kcv; ΔS , deletion of the N terminal slide helix (S) of Kcv; T, turret. Serial dilutions of overnight cultures were spotted onto solid medium plates containing 0.5, 1, 4 and 100 mM K^+ and exposed either to dark (black square) or blue light (447 ± 10 nm, $2 \pm 0.2 \mu W/mm^2$) (blue square). Images were taken after 3 days. Boxed is the LK construct, which was selected for further improvement. (C) Yeast growth complementation with light-gated channel candidates in liquid medium. $\Delta trk1 \Delta trk2$ potassium transport deficient yeast transformed with a selection of the constructs above (K, KL, LK and KLK) was grown in liquid medium in dark and blue light. The medium contained 4, 7, 10 and 100 mM KCl, shown by increasing grey-levels. The four bars of the same color indicate, from left to right, the values of the OD_{600} ratio $[(light/dark)-1]$ measured after 21 h, 45 h, 52 h and 117 h.

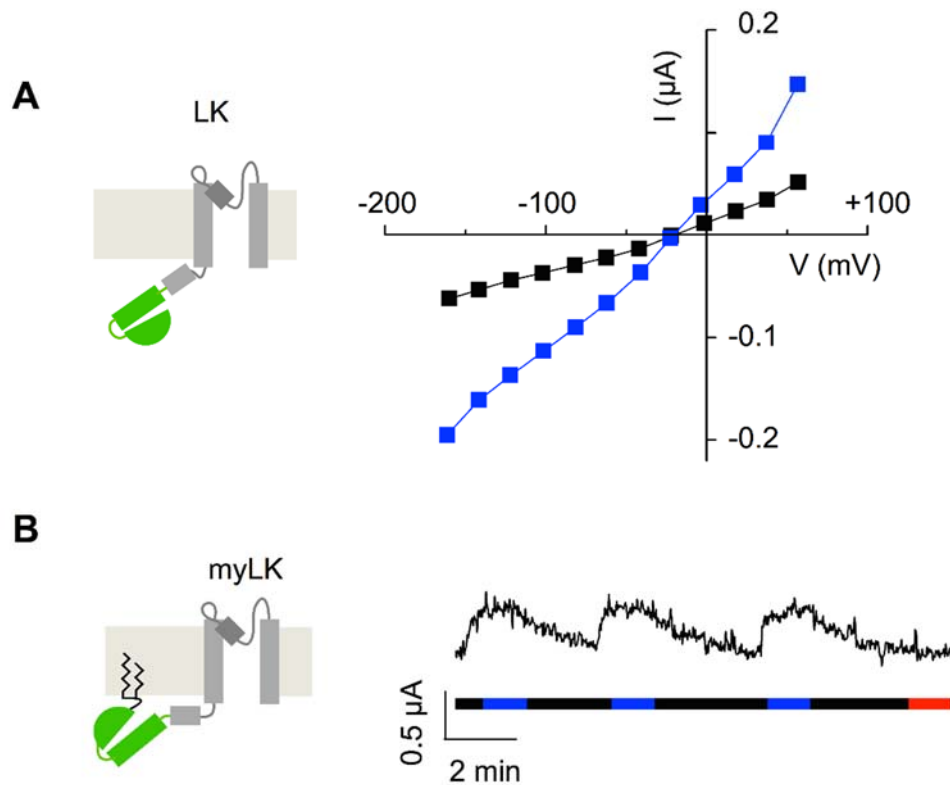


Figure S2. Current recordings from LK and myLK channels in dark and light.

(A) Cartoon representation and current-voltage relationship of LK recorded in *Xenopus* oocyte in the dark (■) and after 10 min of blue light (455 nm, 80 $\mu\text{W}/\text{mm}^2$) (■). External solution contained 50 mM $[\text{K}^+]_{\text{out}}$. (B) Cartoon of myLK with the N-terminal myristoylation and palmitoylation sequence. Continuous current recording at -60 mV in 50 mM $[\text{K}^+]_{\text{out}}$ from one oocyte expressing myLK. The oocyte was exposed to dark/light cycles, including blue light (455 nm) and red light (617 nm).

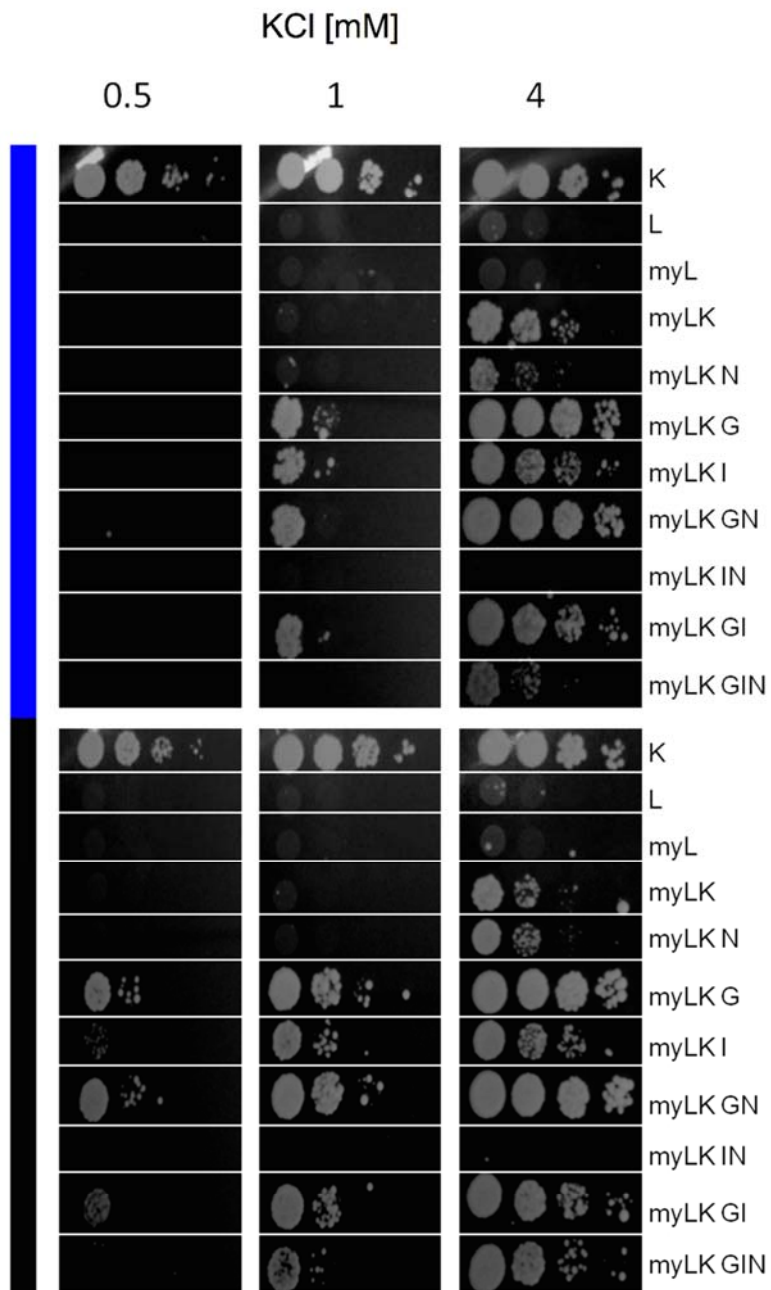


Figure S3. Impact of mutations introduced in myLK on functional complementation of yeast. Mutations introduced in the $J\alpha$ region of myLK were: G528A, I532A and N538A (in short GIN). For functional complementation details see fig. S1B.

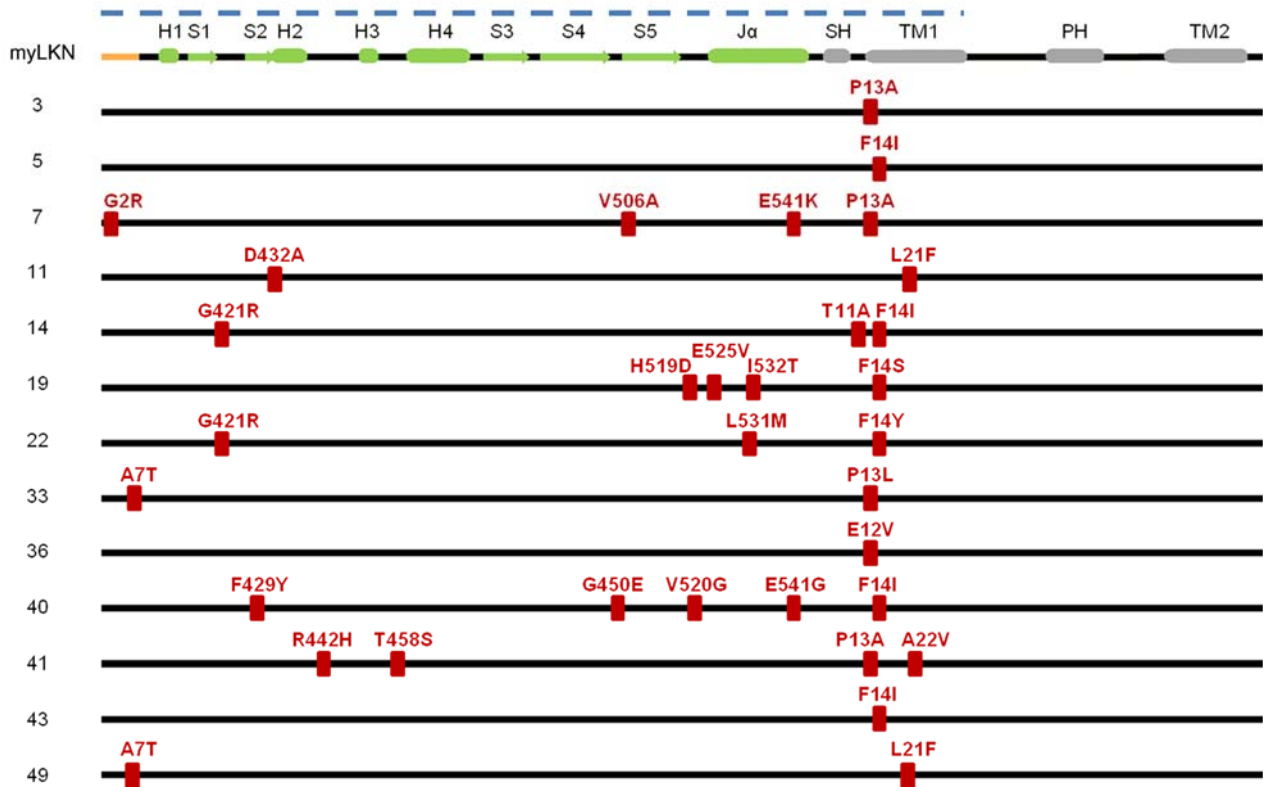


Figure S4. List of clones retrieved from library screening

List of 13 clones selected from a library of myLKN538A (myLKN) mutants and schematic representation of the mutations found and of their position in the sequence, represented by a black line. Colored elements, indicated on the myLKN sequence, are as follow: orange, myristoylation and palmytoylation sequence; green, secondary structures of LOV domain (H1-H4, α helices; S1-S5, beta sheets and $J\alpha$); grey, secondary structures of Kcv (SH, TM1, PH, TM2, see fig. 1A). Dotted line marks the randomized portion of the channel. LOV mutations are numbered on NPH1.1 sequence (AAC05083.1), while those on Kcv are numbered on PBCV-1-Kcv sequence (NP_048599.1).

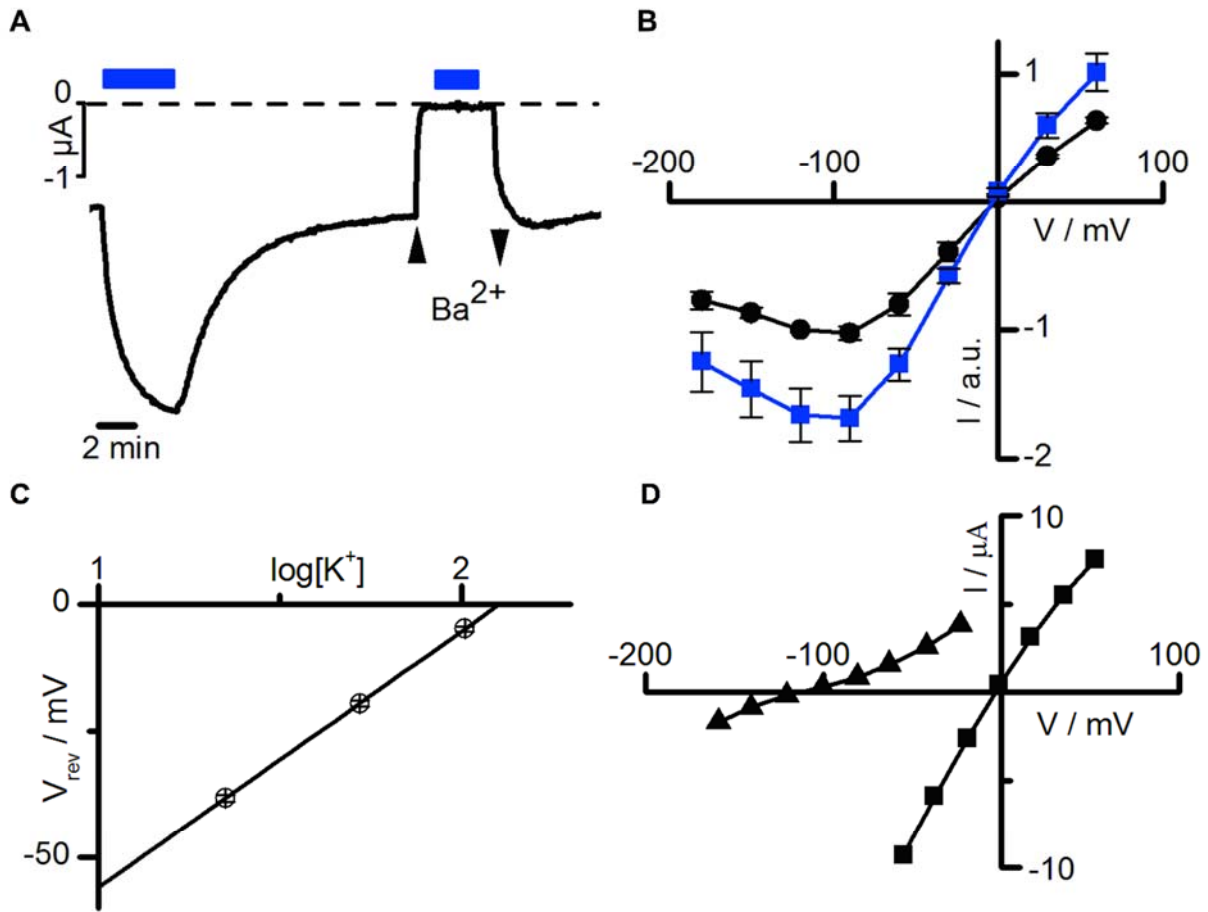


Figure S5. Electrophysiological properties of myLK33 in *Xenopus* oocytes

(A) Effect of blue light on the inward current recorded from one oocyte expressing myLK33, at -80 mV in 50 mM $[K^+]_{out}$. Dotted line indicates zero current level. Bars indicate illumination with blue light (40 $\mu W/mm^2$). Arrowheads indicate addition and removal of 1 mM $BaCl_2$ from the solution. (B) Mean I/V relationship obtained from $n=5$ oocytes: (●) dark, (■) light. Values normalized to the dark current at -120 mV are expressed in arbitrary units (a.u.). (C) Nernst plot with V_{rev} shown as a function of $[K^+]_{out}$ calculated assuming $[K^+]_{in} = 110$ mM (11). Regression line has a slope of -51 mV per log unit $[K^+]_{out}$. (D) I/V curves around V_{rev} of the photocurrent recorded either in 100 mM $[KCl]_{out}$ (■) or $[NaCl]_{out}$ (▲).

myLK	DGTEHV	RDAAEREGVMLIKKTAENIDEAAKEL	VFSKFLTRTEPFMIHL
myLJSK	DGTEHV	RDAAEREGVMLIKKTAE-----	VFSKFLTRTEPFMIHL
myLK Δ6	DGTEHV	RDAAEREGVMLIKKTAENIDEAAKEL	-----TRTEPFMIHL
myLK Δ9	DGTEHV	RDAAEREGVMLIKKTAENIDEAA--	-----TRTEPFMIHL
myLJ21SK	DGTEHV	RDAAEREGVMLIKKTAENIDEAA--	-----KFLTRTEPFMIHL
myLJ18SK	DGTEHV	RDAAEREGVMLIKKTAENID----	-----KFLTRTEPFMIHL
myLJK	DGTEHV	RDAAEREGVMLIKKTAENIDEAAK--	-----TEPFMIHL
myLKd (A523-K6)	DGTEHV	RD-----	-----FLTRTEPFMIHL
myLSK	DGTEHV	RD-----	LVFSKFLTRTEPFMIHL
myLTKdr	DGTEHV	RD-----	-----RTEPFMIHL
myLTKdp	DGTEHV	RD-----	-----PFMIHL
myLTKep	DGTE	-----	-----PFMIHL
myLJSKd(A542-K6)	DGTEHV	RDAAEREGVMLIKKTAENIDE--	-----FLTRTEPFMIHL
myLJSKd(N538-K6)	DGTEHV	RDAAEREGVMLIKKTAE-----	-----FLTRTEPFMIHL

Ja
SH

Figure S6. Modification of the linker sequence connecting the myL domain to Kcv

List of myLK clones and their amino acid sequences showing the modifications introduced in the linker region connecting Ja (residues 523-543 of LOV) (green) to the slide helix (SH, residues 3-12 of Kcv) (grey). The three central residues lysine, glutamate and leucine (KEL), belong to a short loop that follows Ja in LOV. Leucine (pink) is also the starting amino acid of Kcv sequence, after removal of the initial methionine.

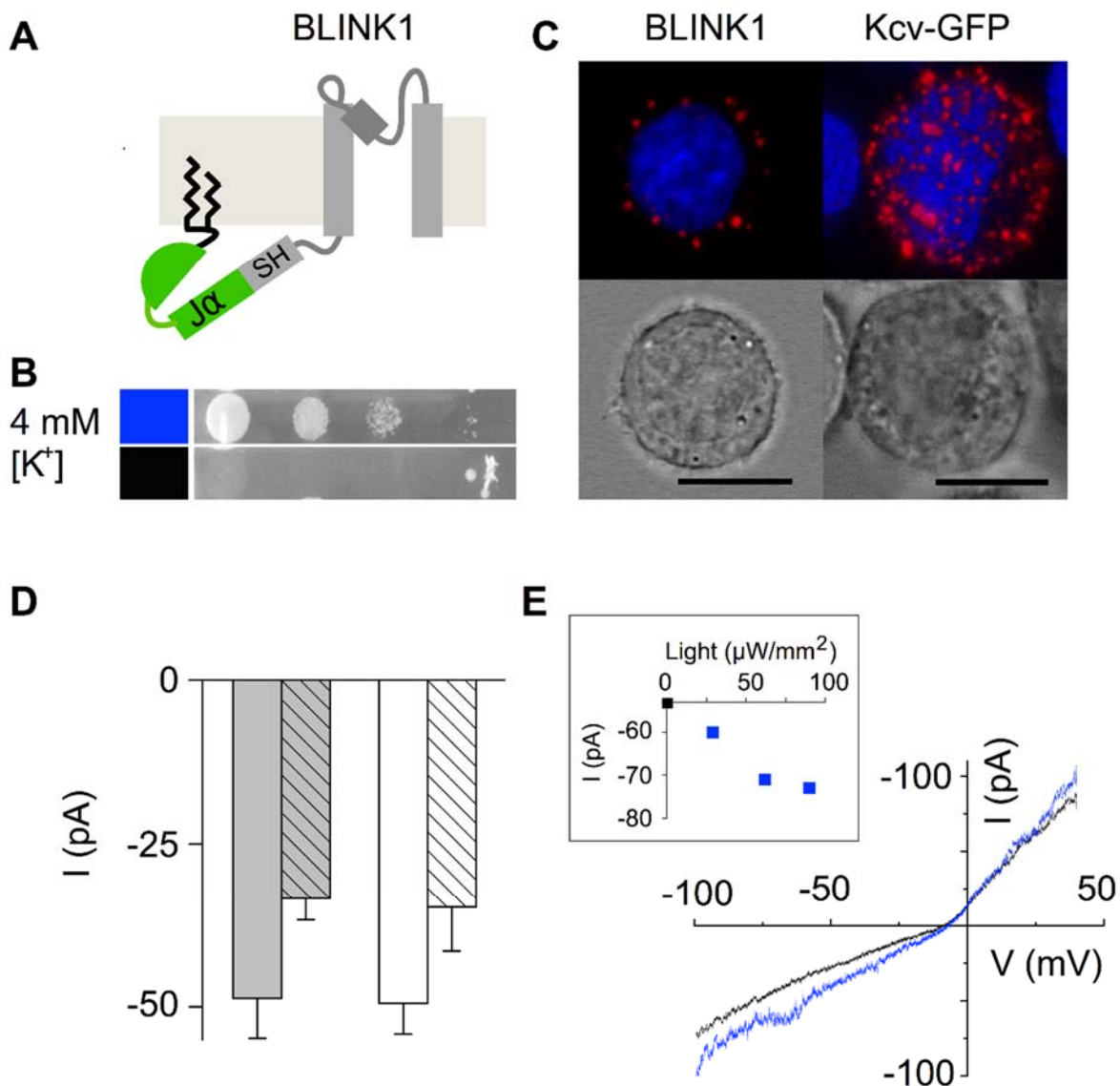


Figure S7. BLINK1 expression in yeast and in HEK293T cells

(A) Cartoon representation (for details see fig. S6) of myLJSK=BLINK1 showing Ja connected to the slide helix (SH) of Kcv; (B) yeast functional complementation by BLINK1 performed as described in fig. S1B. The phenotype shown was observed in 50% of 10 independent experiments. (C) Immunolocalization performed on non-permeabilized HEK293T cells with anti-Kcv monoclonal antibody recognizing specifically the tetrameric form of the channel (30). Left, cells transfected with BLINK1; right: cells transfected with Kcv-GFP. Calibration bar: 10 μm . Fluorescent images show secondary antibody (conjugated to Alexa 594) in red and Hoechst staining of nuclei in blue. Lower panels show corresponding bright field images. (D) Currents recorded in the dark from HEK293T cells ($n = 4$) transfected with BLINK1 + GFP (white) or GFP alone ($n = 8$) (grey). Black diagonal pattern indicates the addition of 1 mM BaCl₂ to the external solution. Measurements were performed at -80 mV in 100 mM [K⁺]_{out}. (E) I/V recorded from a HEK293T cell expressing BLINK1 in dark (black line, average of three subsequent ramps) and blue light (blue line, 455 nm, 90 $\mu\text{W}/\text{mm}^2$). Inset: increase in BLINK1 current recorded at -80 mV, as a function of increasing blue light intensity.

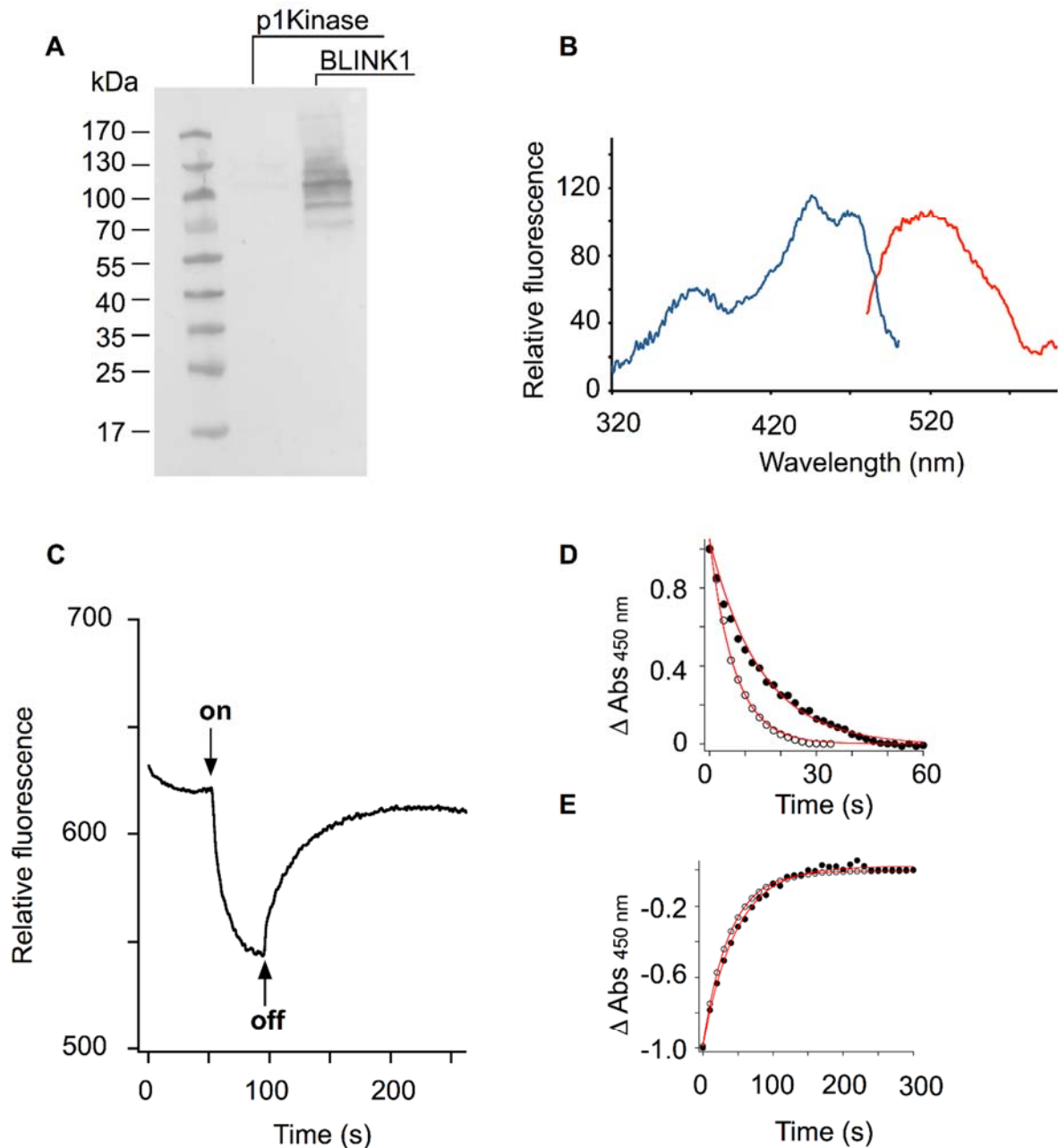


Figure S8. Expression and photochemical characterization of BLINK1 in insect cells.

(A) Immunoblot analysis on Sf9 insect cells infected with either recombinant baculovirus expressing BLINK1 or the kinase domain of Arabidopsis phototropin 1 (p1Kinase) as a negative control. Molecular weight obtained for BLINK1 is consistent with the tetrameric form of the protein (106.5 kDa). (B) Corrected fluorescence excitation (blue line) and emission (red line) spectra for insect cells expressing BLINK1. Spectra were obtained by subtracting control spectra (from cells expressing p1Kinase). (C) Representative light-induced changes in fluorescence emission (520 nm) observed for insect cells expressing BLINK1 following blue light irradiation (on; 455 nm, 90 μ W/mm²) and after irradiation (off). (D) Photoadduct formation for BLINK1 (black circles) shows exponential kinetics (τ = 14.5 s) similar to that obtained for myL (open circles). (E) Photoadduct decay for BLINK1 (black circles) shows exponential kinetics (τ = 51 s) similar to that of for myL (open circles). Data of myL are redrawn from Fig. 1.

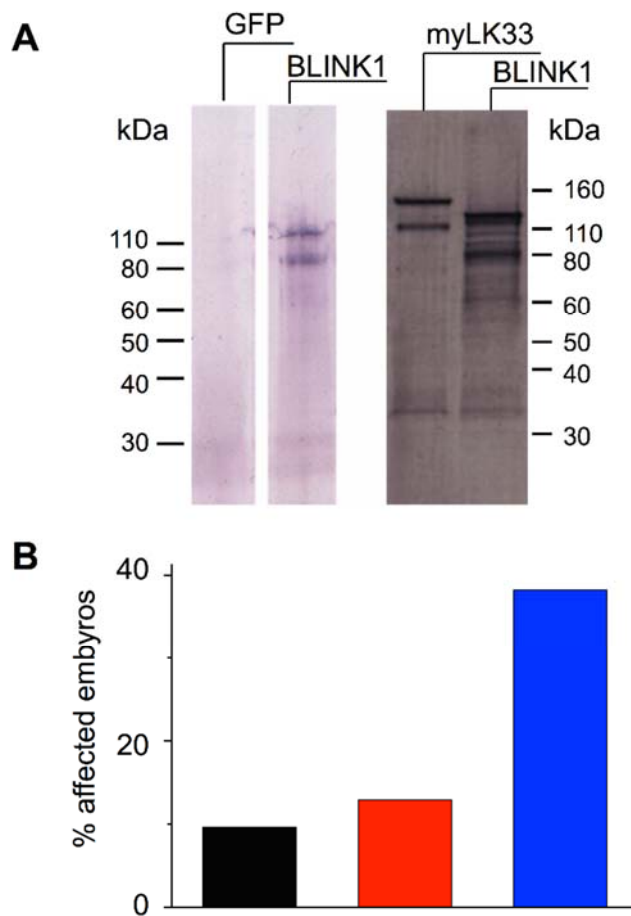


Figure S9. BLINK1 protein expression and absence of red light effect on zebrafish embryos

(A) Western blot analysis performed with an anti-Kcv antibody that recognizes the tetrameric conformation only of the channel (30). Left blot, zebrafish lysates expressing GFP or BLINK1; right blot, yeast microsomes expressing myLK33 or BLINK1. Numbers on the side indicate molecular weights in kDa. Expected m.w of BLINK1 is 106.5 kDa and of myLK33 is 110.5 kDa.

(B) Altered escape response in 3 day-old zebrafish, expressing BLINK1. The embryos (n=34) were tested for escape response with the following protocol: the fish were first kept for 1h in the dark (black) then illuminated for 45 min with red light (617 nm, 80 $\mu\text{W}/\text{mm}^2$) (red) and finally for 45 min with blue light (80 $\mu\text{W}/\text{mm}^2$) (blue). The escape response was tested at the end of each illumination period by gentle mechanical stimulation with a pipette tip (see Movie S1).



Movie S1. Touch response of zebrafish embryos expressing BLINK1.

(GFP) 2 day-old control embryo (GFP-injected), exposed to blue light for 1 h and then tested by mechanical stimulation with the tip of a pipette. (BLINK1) BLINK1-injected embryo, same treatment as the GFP-injected one.

References and Notes

1. S. B. Long, E. B. Campbell, R. Mackinnon, Crystal structure of a mammalian voltage-dependent Shaker family K⁺ channel. *Science* **309**, 897–903 (2005). [Medline doi:10.1126/science.1116269](#)
2. R. Latorre, F. J. Morera, C. Zaelzer, Allosteric interactions and the modular nature of the voltage- and Ca²⁺-activated (BK) channel. *J. Physiol.* **588**, 3141–3148 (2010). [Medline doi:10.1113/jphysiol.2010.191999](#)
3. U. M. Ohndorf, R. MacKinnon, Construction of a cyclic nucleotide-gated KcsA K⁺ channel. *J. Mol. Biol.* **350**, 857–865 (2005). [Medline doi:10.1016/j.jmb.2005.05.050](#)
4. C. Arrigoni, I. Schroeder, G. Romani, J. L. Van Etten, G. Thiel, A. Moroni, The voltage-sensing domain of a phosphatase gates the pore of a potassium channel. *J. Gen. Physiol.* **141**, 389–395 (2013). [Medline doi:10.1085/jgp.201210940](#)
5. M. R. Banghart, M. Volgraf, D. Trauner, Engineering light-gated ion channels. *Biochemistry* **45**, 15129–15141 (2006). [Medline doi:10.1021/bi0618058](#)
6. M. Banghart, K. Borges, E. Isacoff, D. Trauner, R. H. Kramer, Light-activated ion channels for remote control of neuronal firing. *Nat. Neurosci.* **7**, 1381–1386 (2004). [Medline doi:10.1038/nm1356](#)
7. H. Janovjak, S. Szobota, C. Wyart, D. Trauner, E. Y. Isacoff, A light-gated, potassium-selective glutamate receptor for the optical inhibition of neuronal firing. *Nat. Neurosci.* **13**, 1027–1032 (2010). [Medline doi:10.1038/nn.2589](#)
8. J. Y. Kang, D. Kawaguchi, I. Coin, Z. Xiang, D. D. O’Leary, P. A. Slesinger, L. Wang, In vivo expression of a light-activatable potassium channel using unnatural amino acids. *Neuron* **80**, 358–370 (2013). [Medline doi:10.1016/j.neuron.2013.08.016](#)
9. D. Schmidt, P. W. Tillberg, F. Chen, E. S. Boyden, A fully genetically encoded protein architecture for optical control of peptide ligand concentration. *Nat. Commun.* **5**, 3019 (2014). [Medline doi:10.1038/ncomms4019](#)
10. J. M. Christie, Phototropin blue-light receptors. *Annu. Rev. Plant Biol.* **58**, 21–45 (2007). [Medline doi:10.1146/annurev.arplant.58.032806.103951](#)
11. B. Plugge, S. Gazzarrini, M. Nelson, R. Cerana, J. L. Van Etten, C. Derst, D. DiFrancesco, A. Moroni, G. Thiel, A potassium channel protein encoded by chlorella virus PBCV-1. *Science* **287**, 1641–1644 (2000). [Medline doi:10.1126/science.287.5458.1641](#)
12. J. M. Christie, J. Gawthorne, G. Young, N. J. Fraser, A. J. Roe, LOV to BLUF: Flavoprotein contributions to the optogenetic toolkit. *Mol. Plant* **5**, 533–544 (2012). [Medline doi:10.1093/mp/sss020](#)
13. F. C. Chatelain, S. Gazzarrini, Y. Fujiwara, C. Arrigoni, C. Domigan, G. Ferrara, C. Pantoja, G. Thiel, A. Moroni, D. L. Minor Jr., Selection of inhibitor-resistant viral potassium channels identifies a selectivity filter site that affects barium and amantadine block. *PLOS ONE* **4**, e7496 (2009). [Medline doi:10.1371/journal.pone.0007496](#)

14. C. Aicart-Ramos, R. A. Valero, I. Rodriguez-Crespo, Protein palmitoylation and subcellular trafficking. *Biochim. Biophys. Acta* **1808**, 2981–2994 (2011). [Medline doi:10.1016/j.bbamem.2011.07.009](#)
15. D. Strickland, X. Yao, G. Gawlak, M. K. Rosen, K. H. Gardner, T. R. Sosnick, Rationally improving LOV domain-based photoswitches. *Nat. Methods* **7**, 623–626 (2010). [Medline doi:10.1038/nmeth.1473](#)
16. B. Hertel, S. Tayefeh, T. Kloss, J. Hewing, M. Gebhardt, D. Baumeister, A. Moroni, G. Thiel, S. M. Kast, Salt bridges in the miniature viral channel Kcv are important for function. *Eur. Biophys. J.* **39**, 1057–1068 (2010). [Medline doi:10.1007/s00249-009-0451-z](#)
17. J. Mattis, K. M. Tye, E. A. Ferenczi, C. Ramakrishnan, D. J. O’Shea, R. Prakash, L. A. Gunaydin, M. Hyun, L. E. Fenno, V. Gradinaru, O. Yizhar, K. Deisseroth, Principles for applying optogenetic tools derived from direct comparative analysis of microbial opsins. *Nat. Methods* **9**, 159–172 (2011). [Medline doi:10.1038/nmeth.1808](#)
18. R. M. Colwill, R. Creton, Imaging escape and avoidance behavior in zebrafish larvae. *Rev. Neurosci.* **22**, 63–73 (2011). [Medline doi:10.1515/rns.2011.008](#)
19. F. Zhang, L. P. Wang, M. Brauner, J. F. Liewald, K. Kay, N. Watzke, P. G. Wood, E. Bamberg, G. Nagel, A. Gottschalk, K. Deisseroth, Multimodal fast optical interrogation of neural circuitry. *Nature* **446**, 633–639 (2007). [Medline doi:10.1038/nature05744](#)
20. X. Han, E. S. Boyden, Multiple-color optical activation, silencing, and desynchronization of neural activity, with single-spike temporal resolution. *PLOS ONE* **2**, e299 (2007). [Medline doi:10.1371/journal.pone.0000299](#)
21. A. Berndt, S. Y. Lee, C. Ramakrishnan, K. Deisseroth, Structure-guided transformation of channelrhodopsin into a light-activated chloride channel. *Science* **344**, 420–424 (2014). [Medline doi:10.1126/science.1252367](#)
22. J. Wietek, J. S. Wiegert, N. Adeishvili, F. Schneider, H. Watanabe, S. P. Tsunoda, A. Vogt, M. Elstner, T. G. Oertner, P. Hegemann, Conversion of channelrhodopsin into a light-gated chloride channel. *Science* **344**, 409–412 (2014). [Medline doi:10.1126/science.1249375](#)
23. S. Tayefeh, T. Kloss, M. Kreim, M. Gebhardt, D. Baumeister, B. Hertel, C. Richter, H. Schwalbe, A. Moroni, G. Thiel, S. M. Kast, Model development for the viral Kcv potassium channel. *Biophys. J.* **96**, 485–498 (2009). [Medline doi:10.1016/j.bpj.2008.09.050](#)
24. E. Huala, P. W. Oeller, E. Liscum, I. S. Han, E. Larsen, W. R. Briggs, *Arabidopsis* NPH1: A protein kinase with a putative redox-sensing domain. *Science* **278**, 2120–2123 (1997). [Medline doi:10.1126/science.278.5346.2120](#)
25. D. L. Minor Jr., S. J. Masseling, Y. N. Jan, L. Y. Jan, Transmembrane structure of an inwardly rectifying potassium channel. *Cell* **96**, 879–891 (1999). [Medline doi:10.1016/S0092-8674\(00\)80597-8](#)
26. J. M. Christie, A. S. Arvai, K. J. Baxter, M. Heilmann, A. J. Pratt, A. O’Hara, S. M. Kelly, M. Hothorn, B. O. Smith, K. Hitomi, G. I. Jenkins, E. D. Getzoff, Plant UVR8

- photoreceptor senses UV-B by tryptophan-mediated disruption of cross-dimer salt bridges. *Science* **335**, 1492–1496 (2012). [Medline doi:10.1126/science.1218091](#)
27. D. G. Gibson, L. Young, R. Y. Chuang, J. C. Venter, C. A. Hutchison 3rd, H. O. Smith, Enzymatic assembly of DNA molecules up to several hundred kilobases. *Nat. Methods* **6**, 343–345 (2009). [Medline doi:10.1038/nmeth.1318](#)
28. W. Tang, A. Ruknudin, W. P. Yang, S. Y. Shaw, A. Knickerbocker, S. Kurtz, Functional expression of a vertebrate inwardly rectifying K⁺ channel in yeast. *Mol. Biol. Cell* **6**, 1231–1240 (1995). [Medline doi:10.1091/mbc.6.9.1231](#)
29. A. Moroni, C. Viscomi, V. Sangiorgio, C. Pagliuca, T. Meckel, F. Horvath, S. Gazzarrini, P. Valbuzzi, J. L. Van Etten, D. DiFrancesco, G. Thiel, The short N-terminus is required for functional expression of the virus-encoded miniature K⁺ channel Kcv. *FEBS Lett.* **530**, 65–69 (2002). [Medline doi:10.1016/S0014-5793\(02\)03397-5](#)
30. G. Romani, A. Piotrowski, S. Hillmer, J. Gurnon, J. L. Van Etten, A. Moroni, G. Thiel, B. Hertel, A virus-encoded potassium ion channel is a structural protein in the chlorovirus *Paramecium bursaria* chlorella virus 1 virion. *J. Gen. Virol.* **94**, 2549–2556 (2013). [Medline doi:10.1099/vir.0.055251-0](#)
31. M. Granato, F. J. van Eeden, U. Schach, T. Trowe, M. Brand, M. Furutani-Seiki, P. Haffter, M. Hammerschmidt, C. P. Heisenberg, Y. J. Jiang, D. A. Kane, R. N. Kelsh, M. C. Mullins, J. Odenthal, C. Nüsslein-Volhard, Genes controlling and mediating locomotion behavior of the zebrafish embryo and larva. *Development* **123**, 399–413 (1996). [Medline](#)